TITLE
ASP Conference Series, Vol. **VOLUME**, **PUBLICATION YEAR**
EDITORS

Cool Star Chromospheres and the Sun

Jeffrey L. Linsky and Seth Redfield

JILA, University of Colorado and NIST, Boulder, CO 80309-0440

Tom Ayres, Alex Brown, and Graham Harper

CASA, University of Colorado, Boulder, CO 80309-0389

Abstract. We are learning a great deal about the chromospheres of cool stars from the excellent spectra provided by the GHRS and STIS instruments on HST, the far ultraviolet spectra from FUSE, and X-ray spectra from Chandra. Ultraviolet spectra of cool stars are extraordinarily rich with emission lines of neutral species, ions up to O VI, Fe XXI, and fluorescent molecular spectra (CO and H_2) in cool giants and pre-main sequence stars. We also describe the thermal and velocity structure of a luminous cool star using α TrA as an example.

1. What is a Chromosphere?

The term "chromosphere" was coined to describe the region above the solar limb that is distinctly red in color during total eclipses. The red light is primarily Hα emission. The term is now used to indicate the region above the top of a stellar photosphere where nonradiative heating processes (either magnetic or acoustic) become important in the energy balance. The effect of this input of energy is to produce either a temperature rise that eventually leads to nearly complete ionization of hydrogen or a region of cool gas with a very extended scale height supported by turbulence or acoustic waves. Both types of chromospheres exist on the Sun with regions of strong heating producing bright emission in the Lyman-α, Ca II, Mg II, and Fe II lines, which together are the dominant cooling channels. Where the heating is weak, the chromosphere forms CO molecules that radiate efficiently in the infrared to balance the heating. This cool region has been called the COmosphere (Ayres & Rabin 1996). Late-type stars probably have both types of chromospheres, but the relative importance of the two components depends on the rate of magnetic heating, which is much larger in rapidly rotating stars with strong magnetic fields.

While the entire atmosphere above the photosphere could be loosely called a chromosphere, we call only those regions where hydrogen is partially ionized to be the chromosphere and the higher temperature regions by different names because different physical processes are important. Since hydrogen is nearly completely ionized when temperatures reach 20,000–30,000 K, it is useful to call this the top of the chromosphere. One should not think of the chromosphere as a plane-parallel layer, however, as the solar chromosphere is highly inhomogeneous and structured by the magnetic field. Once hydrogen is nearly completely ionized, mechanical heating produces a steep thermal gradient because there is no cooling channel as effective as hydrogen, and Ca^+, Mg^+, and Fe^+ have disappeared long before hydrogen is ionized. The region of steep thermal gradient is often called the "transition region" and extends to roughly 10^6 K. At higher temperatures, $> 10^6$ K, free-free and bound-bound transitions at X-ray wavelengths and wind expansion become the dominant cooling channels and the region is typically called a "corona." ROSAT X-ray observations show that all dwarf stars of spectral types F–M have coronae, and that F–G giants and active binaries also have coronae. In the luminous cool giants and supergiants one typically sees evidence for a cool wind and little or no evidence for a corona, but the case for hot gas in the outer atmospheres of these stars is still not settled. A clear understanding of the thermal and dynamical structures, heating mechanisms, and wind acceleration mechanisms in late-type stars requires detailed spectroscopic studies of these stars. Fortunately this is now feasible.

2. A Spectroscopic Survey of Stellar Chromospheres

We have entered the golden age of stellar spectroscopy: we can now obtain and analyze high resolution stellar spectra from optical to X-ray wavelengths. While IUE gave us a taste of the diagnostically rich ultraviolet (1150–3200 Å) spectra for a variety of stars, the beautiful spectra from the GHRS and STIS instruments on HST are providing the valuable details of line shapes and fluxes for an enormous number of atomic and molecular lines. The FUSE satellite is extending the spectral range to include the far-UV (910–1180 Å), and the EUVE satellite has been obtaining spectra in the 70–400 Å range. Chandra and XMM-Newton are now obtaining X-ray spectra of stars for the first time.

Figure 1 shows a STIS spectrum of the Sun-like star ζ Dor (F7 V). This spectrum is representative of slowly rotating, inactive Sun-like dwarf stars for which the brightest UV emission lines are Lyman-α, the Mg II resonance lines (2796, 2803 Å), transition region lines formed at 30,000–150,000 K (C II-IV, N V, and Si III-IV), and the He II 1640 Å line, which could be formed either by collisional excitation in a 10^5 K plasma or by recombination. By contrast, emission lines of neutrals and singly ionized species (e.g., C I, Si II, and Fe II) formed in the chromosphere at 4,000–8,000 K are relatively weak. Even the O I triplet near 1304 Å is weak compared to the nearby C II 1334, 1335 Å lines, and no molecular species are detected. Stars that are more rapidly rotating than the Sun by virtue of their young age or being in tidally synchronous binary systems (e.g., RS CVn systems) show transition region lines with very large surface fluxes approaching the "saturation limit" (cf. Caillault 1996) and also the Fe XXI 1354 Å emission line formed at 10^7 K in the stellar corona (Linsky et al. 1998). Since this is the only coronal line typically seen in UV spectra and STIS has much higher spectral resolution than the X-ray spectrometers on Chandra and XMM-Newton, STIS observations of the Fe XXI line are our prime source for studying stellar coronal dynamics.

More luminous late-type stars show qualitatively different UV spectra. The STIS spectrum (cf. Figure 2) of the prototypical hybrid-chromosphere star α TrA (K2 II-III) shows the same emission lines as ζ Dor, but the collisionally excited

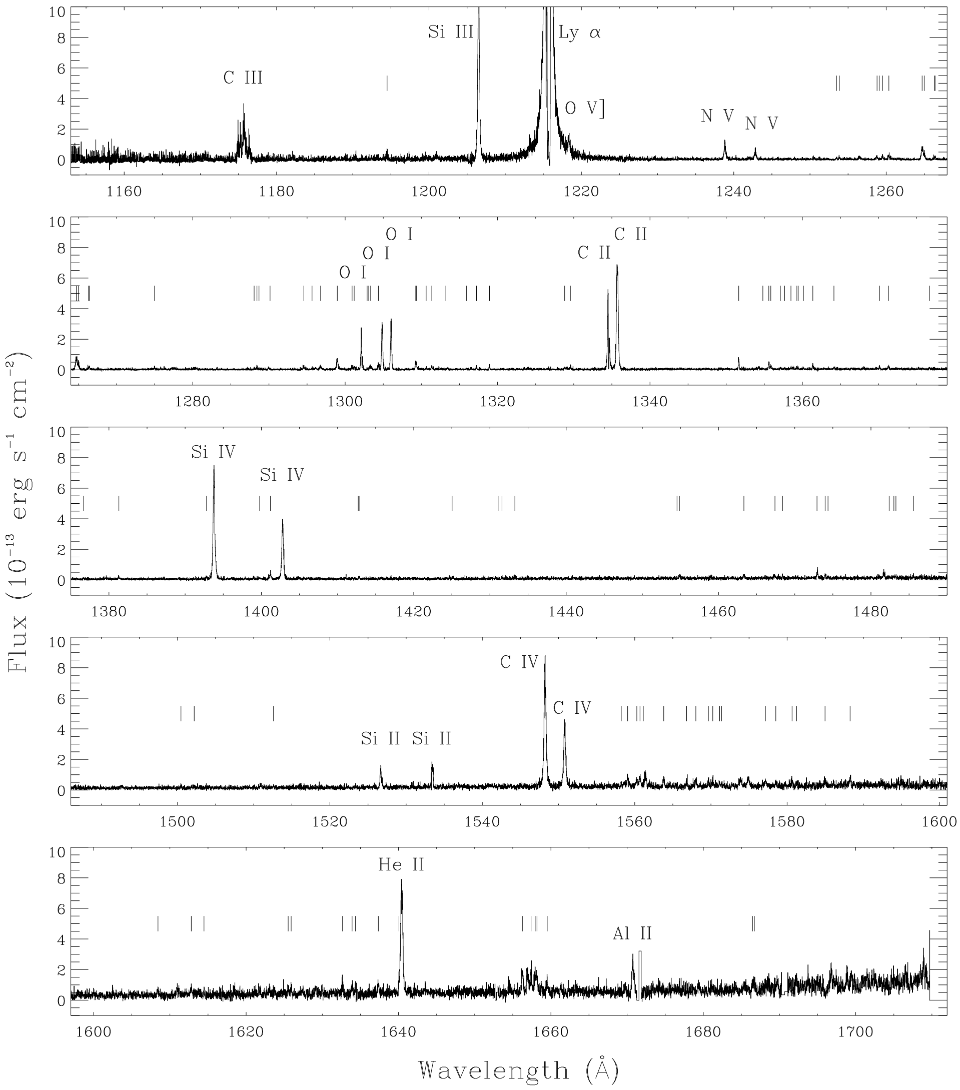

Figure 1. Spectrum of ζ Dor (F7 V) obtained with the STIS E140M grating, which has a resolution $R = \lambda/\Delta\lambda = 45,800$ (6.6 km s^{-1}). Vertical tick marks indicate weak emission lines. From Redfield et al. 2000.

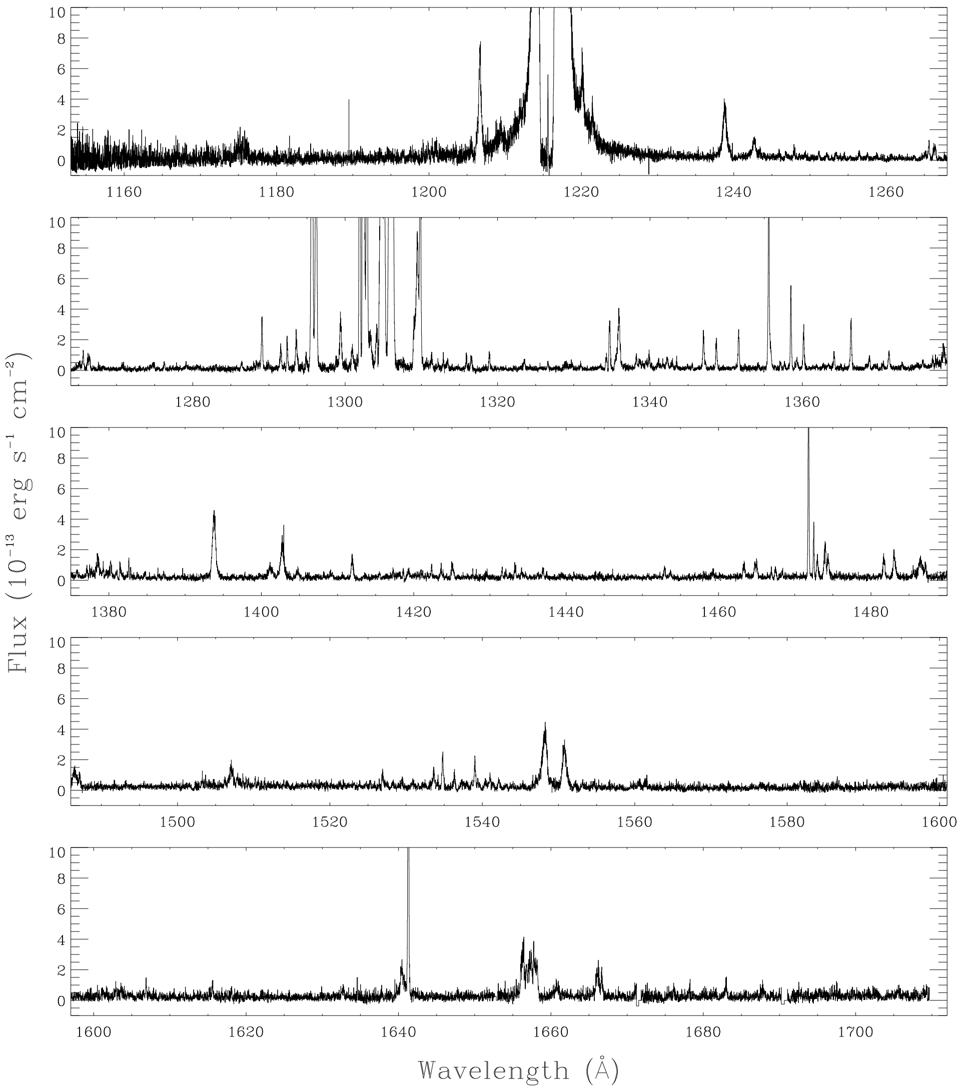

Figure 2. STIS E140M spectrum of α TrA (K2 II-III).

transition region lines are weaker than the fluoresced O I triplet centered at 1304 Å. Other prominent fluorescent features are the O I 1641 Å line, which is brighter than the He II 1640 Å line, and many CO lines located primarily in the 1340–1540 Å region. A number of Fe II lines fluoresced by Lyman-α are present in the FUSE and STIS spectral regions (Harper et al. 2001). This star has a high speed but a variable cool wind described in Section 3.

The UV spectrum of the late-type supergiant λ Vel (K5 Ib-II) is dominated by emission lines of neutral or singly ionized metals that are either fluoresced or show blue-shifted absorption features indicative of a massive low terminal velocity wind ($\sim 3 \times 10^{-9} M_{\odot}$ yr^{-1}, 29–33 km s^{-1}). Figure 3 shows portions of the UV spectrum of λ Vel (Carpenter et al. 1999) with fluoresced O I, S I, Fe II, and Al II lines and a large number of Fe II lines with wind absorption features. Molecular H_2 lines pumped by Lyman-α are seen in STIS spectra of Arcturus (K2 III) (Ayres et al. 2000) and the pre-main sequence K7 V star TW Hya (cf. Fig. 4). Fluorescent H_2 spectra will likely turn out to be common in these star classes as more observations are analyzed.

The FUSE spectral region contains the H I Lyman series from Lyman-β to the series limit near 912 Å, strong lines of C III (977, 1175 Å) and O VI (1032, 1037 Å) formed near 60,000 and 300,000 K, respectively. Emission lines of C I, O I, Fe II, and hotter ions are also found. With a resolution $R \sim 20,000$ (about 15 km s^{-1}), FUSE observations of the O VI lines provide an excellent diagnostic for the dynamics and energy balance in those poorly understood regions of a stellar atmosphere lying just below or next to the corona.

The extreme ultraviolet (EUV) spectral region from 70–400 Å has been studied by the EUVE satellite with a resolution $R = 200$–400 (750–1500 km s^{-1}). This resolution is sufficient to identify the stronger emission lines but does not permit a good separation of the continuum from many weaker lines, nor does it allow one to study coronal dynamics. Nevertheless, EUVE was the first instrument to permit spectral studies of the coronal emission measure distributions and metal abundances. Figure 5 shows a portion of the EUVE spectra of two active binary systems, Capella (G8 III + G1 III) and HR 1099 (K1 IV + G5 V). Both stars show emission lines of Fe IX–XXIII, formed between 8×10^5 K and 2×10^7 K, but the higher stages of ionization are much stronger in the shorter period (2.8 days) and more active HR1099 system. This shows that the emission measure distribution of the coronal plasma in HR1099 extends to much higher temperatures than for Capella, but the coronae in both systems have a broad range of temperatures that could not be readily determined from low resolution X-ray detectors on ROSAT and ASCA.

The X-ray spectrometers on Chandra and XMM are providing the first X-ray spectra of stars other than the Sun. Chandra's High Energy Transmission Grating Spectrometer (HETGS) provides resolutions of 500–1,000, and the Low Energy Transmission Grating Spectrometer (LETGS) provides resolutions of 1,000–2,000. The Reflection Grating Spectrometer (RGS) on XMM-Newton provides resolutions up to 800 with higher throughput than Chandra's spectrometers. Figure 6 shows portions of the the X-ray spectra of Capella and HR1099. This spectral region contains lines from ionization stages as high as Fe XXIV, which is much stronger in HR1099 than Capella. Also shown are the helium-like triplets of Mg XI and Si XIII. The ratio of the forbidden/intersystem

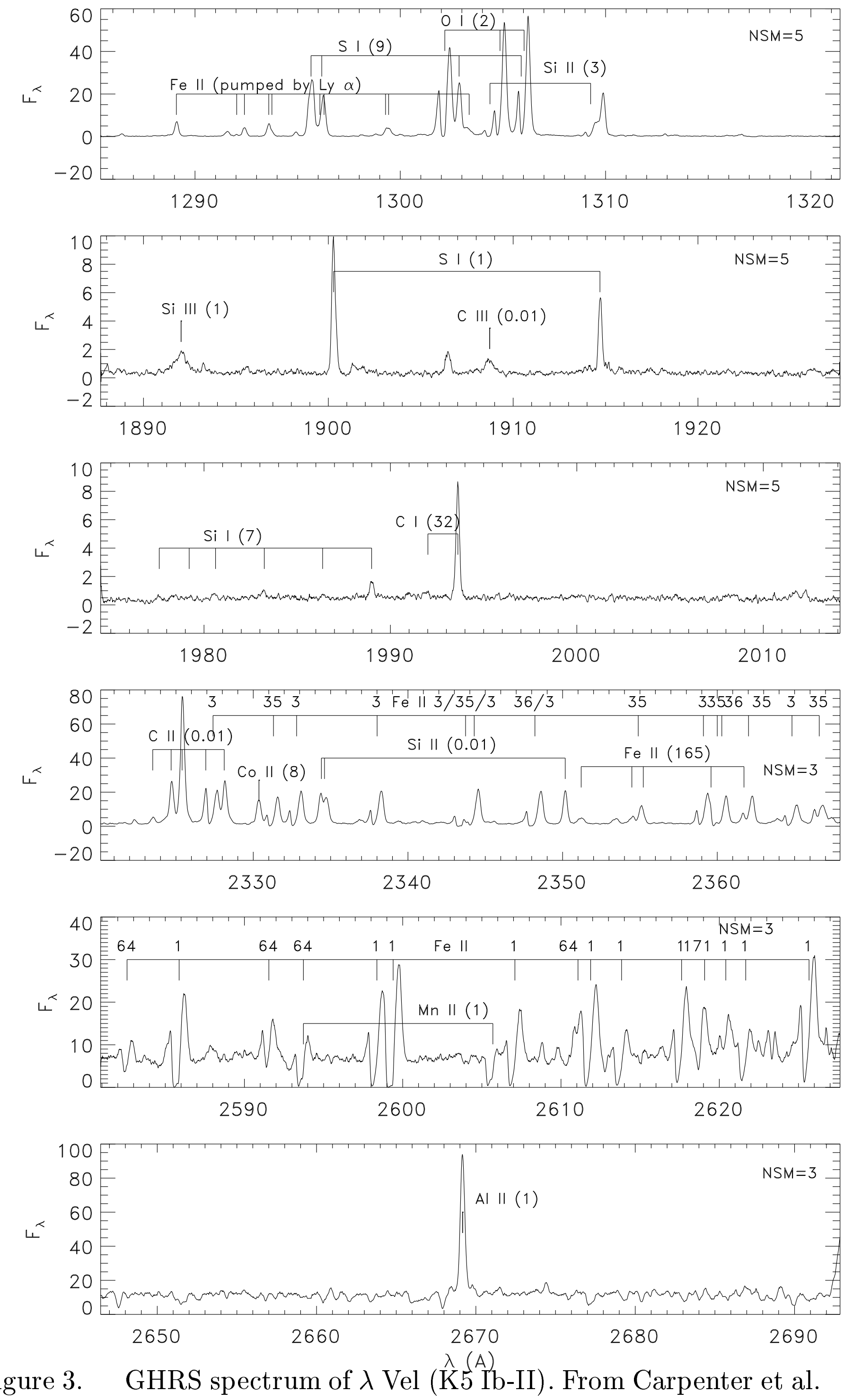

Figure 3. GHRS spectrum of λ Vel (K5 Ib-II). From Carpenter et al. 1999.

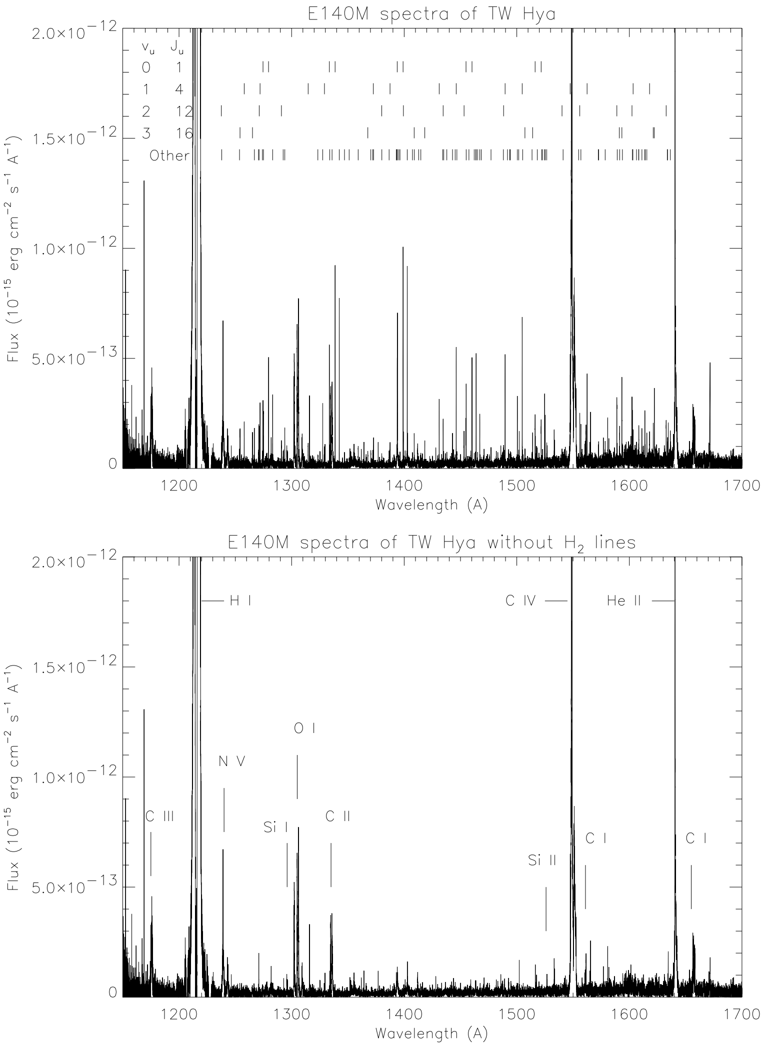

Figure 4. (top) STIS spectrum of TW Hya. (bottom) Same spectrum with the H_2 lines removed.

lines in these triplets indicate a coronal density of $n_e \approx 10^{11}$ cm^{-3} in Capella's corona (Brinkman et al. 2000; Ayres et al. 2001). The spectral resolution and wavelength stability of the HETGS are good enough that Doppler shifts clearly show that the bulk of the coronal emission in the HR1099 system is from the K1 IV star. Doppler shifts of coronal emission lines during flares have not yet been seen but will most likely be detected when large flares are observed.

3. Expanding Chromospheres: The Wind of α TrA

We have known for many years that the outer layers of luminous cool stars expand with large mass loss rates, but the thermal and velocity structure of the winds could not be determined without the excellent high resolution GHRS and STIS spectra that are now available. We are now analyzing spectra of Alpha TrA (K2 II-III), the prototype of the class of hybrid-chromosphere stars.

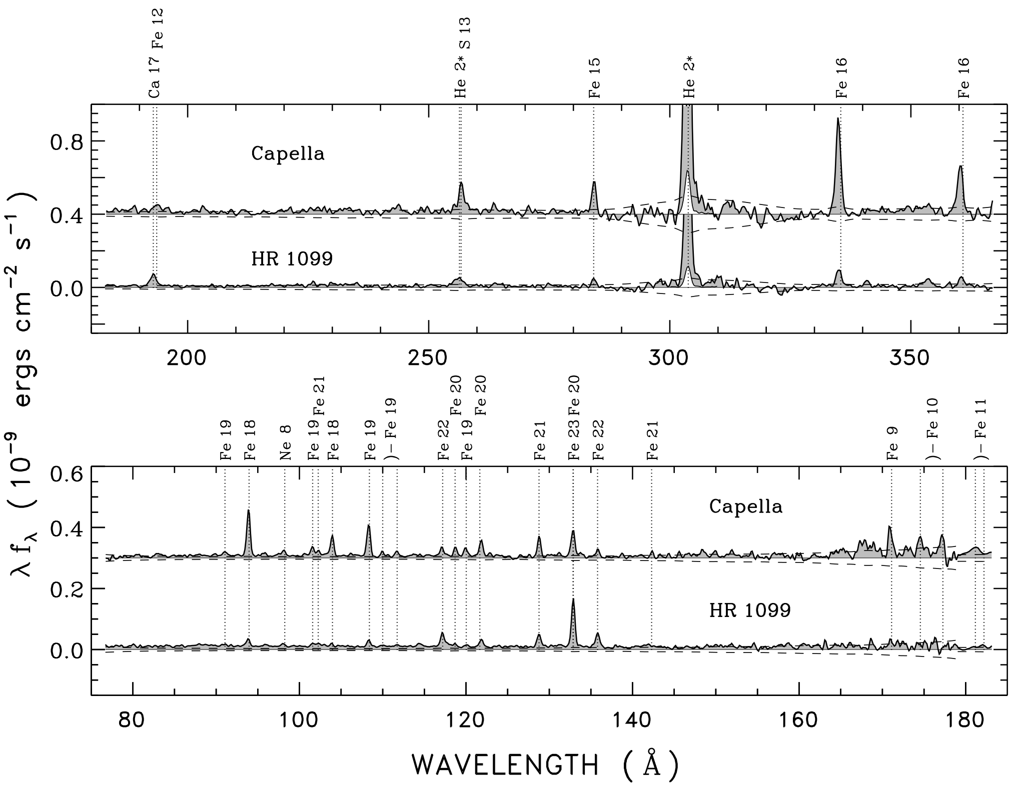

Figure 5. Extreme ultraviolet spectra of Capella and HR1099 observed with the EUVE satellite (Ayres et al. 2001).

This class of stars was first identified by Hartmann et al. (1980) on the basis of having both emission lines formed at 10^5 K and strong winds observed in the chromospheric Mg II h and k lines. The STIS data were reduced using the STIS team software including the ECHELLE-SCAT routine (Lindler 1999) that removes the scattered light, which is important near the Lyman-α line.

The presence of outflowing gas in a stellar wind is identified by blue-shifted absorption features seen in optically thick spectral lines. These lines formed by scattering in a geometrically extended wind show a classic P Cygni shape with both blue-shifted absorption, produced by outflowing gas in front of the star, and extra emission on the red side of the line, produced by scattering from outflowing gas behind (but not occulted by) the star.

Figure 7 shows the Mg II k line plotted in heliocentric velocity for the STIS observation (July 1999) and the two GHRS observations (February 1993 and May 1994). The two deep interstellar absorption features at +3 and -17 km s^{-1} are interstellar. The pre-COSTAR February 1993 spectrum has additional scattered light and lower spectral resolution that is clearly seen in the interstellar features. The profiles at positive velocities are similar in shape although somewhat different in width. At velocities between –30 and –200 km s^{-1}, scattering in the wind in front of the star absorbs much of the Mg II emission from the stellar chromosphere, although the amount of opacity is a function of velocity and time. The profiles of the Mg II h (2803 Å) and k (2796 Å) lines in the

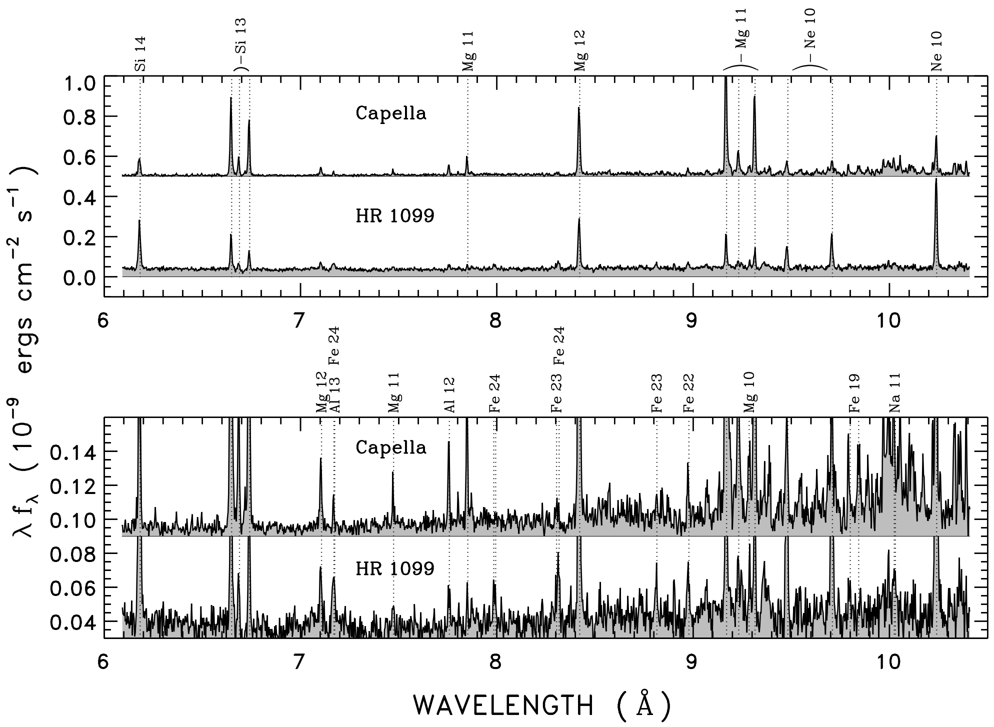

Figure 6. A portion of the X-ray spectra of Capella and HR1099 observed with the High Energy Transmission Grating Spectrometer on Chandra. The bottom panel shows the same spectra as the top panel but with an expanded flux scale (from Ayres et al. 2001).

July 1999 data set are very similar out to the end of the wind absorption near –200 km s^{-1}, demonstrating that the wind opacity is structured.

In Figure 8 we plot the empirical wind optical depth τ_{-v} as a function of velocity for the Mg II h and k lines. We estimate the optical depth from $\tau_{-v} = ln[f_{+v}/f_{-v}]$, with f_{+v} is the flux on the red side of the line where there is no wind absorption and f_{-v} is the observed flux at the same velocity on the blue side. Velocity points are deleted when a flux is $< 2\sigma$ above zero. This simple method overestimates the optical depth because the red side of the line includes photons scattered from behind the star. We have flipped the Mg II lines about zero velocity (heliocentric), but using the stellar radial velocity of –3.3 km s^{-1} produces minimal changes. The structure of the h line tracks the k line at all velocities, confirming that no other spectral lines are absorbing the wind. We also plot twice the Mg II h line opacity to compare the column density in the two lines that differ in oscillator strength by a factor of 2. Between –80 and –200 km s^{-1}, the column densities are very similar with narrow peaks at –100 and –130 km s^{-1} and a broad peak centered near –165 km s^{-1}.

Figure 9 shows the same optical depth and column density plots for the February 1993 data. The results are very different from the July 1999 data (Figure 8). In the 1993 and May 1994 data the wind opacity extends only to about –130 km s^{-1} and opacity plots rather than the column density plots of

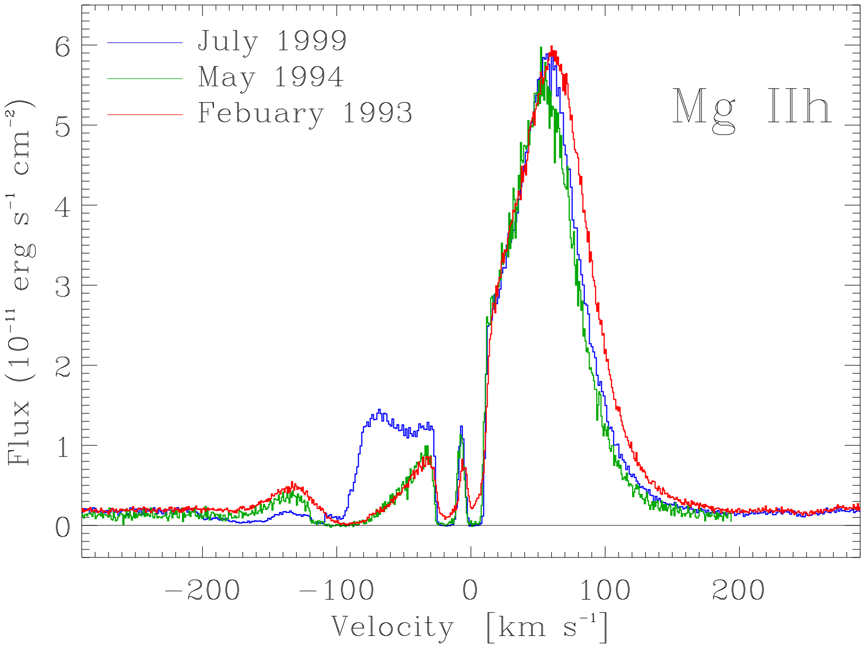

Figure 7. Observed profiles of the α TrA Mg II h line.

the two line agree. Which of these profiles is typical for α TrA? IUE obtained high resolution echelle spectra of the Mg II lines in α TrA on at least 32 occasions between 1979 February and 1993 July (a total of 74 individual spectra). While changes in the wind absorption structure are commonly seen in hybrid-chromosphere stars, a high speed wind profile shape like the STIS α TrA profile was observed only once before (IUE spectrum LWR13982 obtained on 1982 August 19). All other IUE spectra look similar to the 1993 and 1994 GHRS spectra.

In their wind model constructed to fit the 1993 February 10 data set, Harper et al. (1995) derived a terminal velocity of 100 km s^{-1}, turbulent velocity of 24 km s^{-1}, and $\dot{M} \geq 1.8 \times 10^{-10} \frac{\mathrm{A(Mg)}}{\mathrm{A(Mg\ II)}} M_{\odot} \mathrm{yr}^{-1}$. We have not yet computed a model to fit the 1999 July 23 data, but inspection of Figures 3 and 4 show that in July 1999 the wind had an unusually high speed with a terminal velocity near 200 km s^{-1} and far less absorption at –30 to –80 km s^{-1} compared to the 1994, 1993, and all but one of the earlier IUE spectra.

Is the wind opacity structure similar at higher ionization temperatures to what is seen in the Mg II lines created between 5,000–10,000 K? The wind opacity in the O I lines ends at about –80 km s^{-1}. The C II and Si III lines show a very similar opacity structure to Mg II with the opacity extending out to about –200 km s^{-1}. The C II line even shows the double peak structure near –100 and –130 km s^{-1}. The Si IV, C IV, and N V lines show no obvious wind opacity, indicating that the wind has a low ionization temperature.

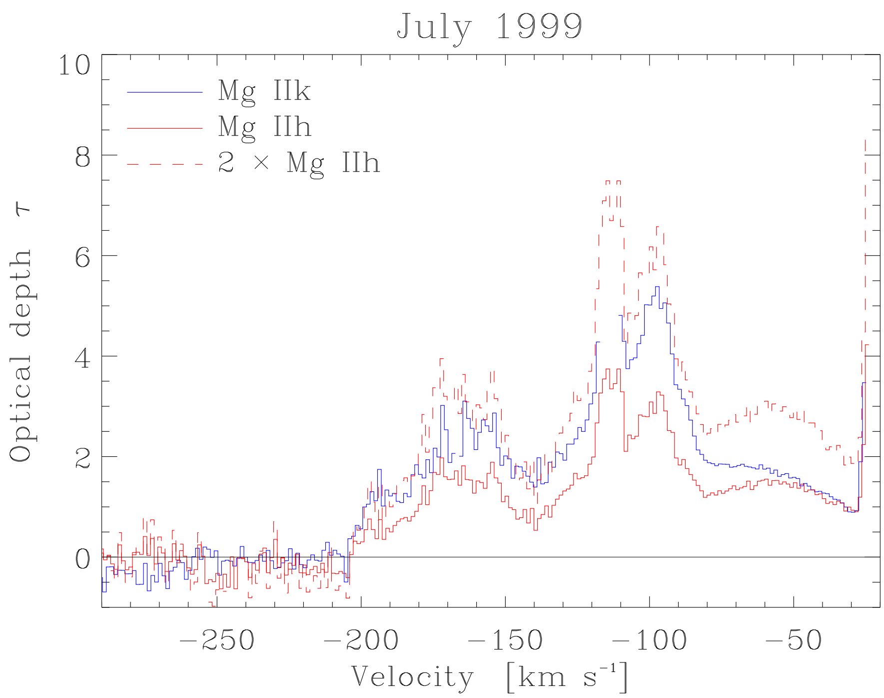

Figure 8. Optical depths in the α TrA Mg II h and k lines.

On the basis of the relative opacity of the Si III and Mg II lines but no opacity in the Si IV lines, we estimate that the maximum wind temperature lies in the range 17,000–20,000 K. There is no significant wind opacity in lines formed near 10^5 K in α TrA. This detailed analysis of the wind of α TrA provides clear guidance for modelling the winds of cool luminous stars. The expanding gas has relatively low ionization, is time variable, and the velocity distribution can be highly structured.

Acknowledgments. Our analysis of HST, Chandra, and FUSE data is supported by NASA grants S-56500-D and H-04630D to the University of Colorado and NIST and grants via Johns Hopkins University.

References

Ayres, T.R., Brown, A., Osten, R.A., Huenemoerder, D.P., Drake, J.J., Brickhouse, N.S., & Linsky, J.L. 2001, ApJ, in press

Ayres, T.R., et al. 2000, in ASP Conf. Ser., Cool Stars, Stellar Systems, and the Sun, ed. J. Garcia Lopez, R. Rebolo, & M.R. Zapatero Osorio (San Francisco: ASP), in press

Ayres, T.R., & Rabin, D. 1996, ApJ, 460, 1042

Brinkman, A.C., et al. 2000, ApJL, 530, L111

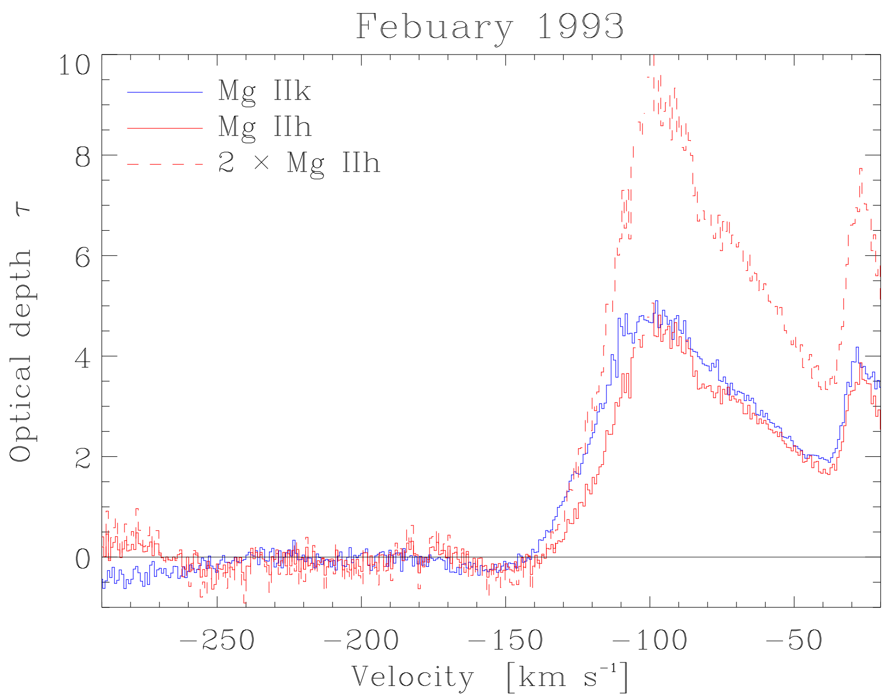

Figure 9. Optical depths in the α TrA Mg II h and k lines.

Caillault, J.-P. 1996, in ASP Conf. Ser. Vol. 109, ed. R. Pallavicini & A.K. Dupree (San Francisco: ASP), 325

Carpenter, K.G., Robinson, R.D., Harper, G.M., Bennett, P.D., Brown, A., & Mullan, D.J. 1999, ApJ, 521, 382

Harper, G.M., Wilkinson, E., Brown, A., Jordan, C., & Linsky, J.L. 2001, ApJ, submitted

Harper, G.M., Wood, B.E., Linsky, J.L., Bennett, P.D., Ayres, T.R., & Brown, A. 1995, ApJ, 452, 407

Hartmann, L., Dupree, A.K., & Raymond, J.C. 1980, ApJL, 236, L143

Lindler, D., 1999, CALSTIS Reference Guide (Greenbelt: NASA/LASP)

Linsky, J.L., Wood, B.E., Brown, A., & Osten, R.A. 1998, ApJ, 492, 767

Redfield, S., Linsky, J.L., Ayres, T.R., & Brown, A. 2000, in ASP Conf. Ser., Cool Stars, Stellar Systems, and the Sun, ed. J. Garcia Lopez, R. Rebolo, & M.R. Zapatero Osorio (San Francisco: ASP), in press